

# RSC Advances



This is an *Accepted Manuscript*, which has been through the Royal Society of Chemistry peer review process and has been accepted for publication.

*Accepted Manuscripts* are published online shortly after acceptance, before technical editing, formatting and proof reading. Using this free service, authors can make their results available to the community, in citable form, before we publish the edited article. This *Accepted Manuscript* will be replaced by the edited, formatted and paginated article as soon as this is available.

You can find more information about *Accepted Manuscripts* in the [Information for Authors](#).

Please note that technical editing may introduce minor changes to the text and/or graphics, which may alter content. The journal's standard [Terms & Conditions](#) and the [Ethical guidelines](#) still apply. In no event shall the Royal Society of Chemistry be held responsible for any errors or omissions in this *Accepted Manuscript* or any consequences arising from the use of any information it contains.

Cite this: DOI: 10.1039/c0xx00000x

www.rsc.org/xxxxxx

## ARTICLE TYPE

# The Amorphous Phase Formation in the Carbothermal Reduction and Nitridation Route to $\text{SrSi}_2\text{O}_2\text{N}_2\text{:Eu}^{2+}$ : A New Clue to Understand the Catalytic Effect of Carbon on the Synthesis of $\text{Sr}_2\text{Si}_5\text{N}_8\text{:Eu}^{2+}$ for White Light-emitting Diode

Lei Chen,<sup>a</sup> Shaochan Xue,<sup>a</sup> Xiuling Chen,<sup>a</sup> Erlong Zhao,<sup>a</sup> Jie Deng,<sup>a</sup> Xiaorong Deng,<sup>a</sup> Shifu Chen,<sup>a,b</sup> Yanfang Liu,<sup>c</sup> Yang Jiang,<sup>a</sup> and Heqin Li<sup>a</sup>

Received (in XXX, XXX) Xth XXXXXXXXX 20XX, Accepted Xth XXXXXXXXX 20XX

DOI: 10.1039/b000000x

This work gives an explanation for the mechanism of carbothermal reduction contributed to the synthesis of  $\text{Sr}_2\text{Si}_5\text{N}_8\text{:Eu}^{2+}$  nitride phosphor from the viewpoint of heat released and propagated within local region, which makes the actual temperature far higher than its pre-set value in reaction. Two pathways of carbon mixing were designed to synthesize the  $\text{SrSi}_2\text{O}_2\text{N}_2\text{:Eu}^{2+}$  at low temperature. However, the nitride  $\text{Sr}_2\text{Si}_5\text{N}_8\text{:Eu}^{2+}$  was observed in the homogenous mixing of carbon with raw materials, rather placing carbon on bottom, which demonstrated that a close contact (used for heat conduction) of carbon with raw materials was a precondition for nitride formation. Moreover, the presence of an amorphous layer, identified with High-Resolution Transmission-Electron-Microscope, on the surface of phosphor particles provides an essential clue to understand the mechanism of nitridation reaction at relatively low temperature.

## 1. Introduction

Nowadays, The  $\text{Sr}_2\text{Si}_5\text{N}_8\text{:Eu}^{2+}$  was one of the most widely used red phosphor in white light-emitting diode (LED) devices package, by combining with blue LED chip and yellow (or green) phosphor to produce high-quality white light, with amiable colour temperature and colour rendering index.<sup>1-9</sup> However, the commercial available red phosphor of  $\text{Sr}_2\text{Si}_5\text{N}_8\text{:Eu}^{2+}$  generally was synthesized from the precursors of high-purity metal Sr,  $\text{Sr}_3\text{N}_2$ ,  $\text{Si}_3\text{N}_4$ ,  $\text{SrSi}_2$  (alloy),  $\text{Eu}_3\text{N}_2$ , or  $\text{Eu}_2\text{O}_3$ , employing high-temperature at 1500-1700 °C in a graphite-heater gas-pressure furnace or radio frequency furnace.<sup>1-9</sup> Due to the metal Sr and  $\text{Sr}_3\text{N}_2$  are sensitive to moisture and oxygen, the whole processes, including raw materials reserve, mixing, and firing, of synthesis must be kept in inert atmosphere. The expensive nitride precursors, sophisticated equipment, and critical condition required for synthesis make the phosphor costly. However, the rapid popularization of LED makes it has a critical requirement of on the cost of key raw material. Therefore, a facile synthesis is desired.<sup>2-4</sup>

Meanwhile, much effort has been paid to explore the facile synthesis, such as the gas-pressure sintering approach from metal oxides.<sup>3-4</sup>

In previous researches, the carbothermal reduction and nitridation (CRN) reaction route has been proved to be a promising way to obtain  $\text{Sr}_2\text{Si}_5\text{N}_8\text{:Eu}^{2+}$  at relatively low temperature in normal pressure.<sup>7-10</sup> However, the mechanism was still not clear. Recently, a theoretical study on the thermodynamic stabilities of Sr–Si–N–O system based on the first-principle density functional theory calculations shows that the presence of solid carbon helpfully decreases the oxygen partial pressure, providing a fresh standpoint to understand the contribution of carbon to the formation of nitride compounds.<sup>10</sup> Nevertheless, the real effect of carbon on the synthesis of  $\text{Sr}_2\text{Si}_5\text{N}_8\text{:Eu}^{2+}$  was still to be clarified. In this work, two different pathways of carbon mixing were designed to synthesize the green phosphor  $\text{SrSi}_2\text{O}_2\text{N}_2\text{:Eu}^{2+}$ . Besides  $\text{SrSi}_2\text{O}_2\text{N}_2\text{:Eu}^{2+}$ , the phase of  $\text{Sr}_2\text{Si}_5\text{N}_8\text{:Eu}^{2+}$  was obtained at a relatively low temperature of 1400 °C through homogenous mixing carbon with raw materials and the ratio of  $\text{Sr}_2\text{Si}_5\text{N}_8$  to  $\text{SrSi}_2\text{O}_2\text{N}_2$  phases increased with carbon content, which indicates that a close contact of the raw materials with carbon was a necessary condition for the formation of the nitride compound. The presence of an amorphous layer on particles surface, discriminated using the High-Resolution Transmission-Electron-Microscope (HR-TEM), provides a key to understand the mechanism why nitride compounds are easily synthesized with the CRN route.

## 2. Experimental

The SrO, achieved by firing  $\text{SrCO}_3$  (99.9%, Sinopharm, China) at 1200 °C for 2 h,  $\text{Si}_3\text{N}_4$  (99.9%, Ube, Japan),  $\text{Eu}_2\text{O}_3$  (99.99%, AMR, China) were used as the raw materials, and graphite powder (99.85%, Sinopharm, China) was used as carbon source. Two methods of the carbon mixing were implemented: (1) the carbon and raw materials were thoroughly grounded using an agate mortar and then the homogenous mixture was placed into a Mo crucible; (2) carbon was firstly placed at the bottom of the Mo crucible and then the homogenous mixture of the raw materials was filled in the Mo crucible on the top of carbon layer. Then, the crucibles were transferred into a tube furnace, successively fired at 1400 °C for 4 hours in  $\text{N}_2$  atmosphere. The emission and excitation spectra were collected using a fluorescence spectrophotometer (Hitachi, F-4600); the thermal quenching luminescence was recorded using the spectrometer in combination with a heating apparatus. The absorption and the internal and external quantum efficiency of the phosphors were tested with the Half Moon-based Quantum Efficiency Measurement System (Otsuka Electronics, QE-2100) at variant wavelengths excitation. The thermal stability of luminescence and quantum efficiency were compared with the commercially available  $\text{Y}_3\text{Al}_5\text{O}_{12}:\text{Ce}^{3+}$  at 455 nm excitation, which is a most popular way to produce white light in white LEDs. The crystal structures of samples were investigated with XRD analysis using a Rigaku D/Max-rB diffractometer with Cu  $\text{K}\alpha$  radiation, operated at 45 kV and 40 mA. The morphology was characterized using the Field-Emission Transmission-Electron-Microscope (JEOL, JEM-2100F).

## 3. Results and discussions

The phosphor synthesized by layering carbon at the bottom of crucible stratified two layers: the upper green layer and a reddish orange in the substratum. Furthermore, the thickness of the reddish interface increases with the increasing carbon content. Fig.1 (a) presents the emission spectra of the upper green layer under the excitation of 370 nm, in which a broad band with peak at about 545 nm is observed. Under the same excitation wavelength, the emission spectra of the sample synthesized with carbon and raw materials homogenous mixing together comprises of two bands: a dominant peaked at 545 nm and a subsidiary peaked at 632 nm.

Fig. 2 shows the XRD patterns of phosphors prepared (a) in the absence of carbon, (b) with carbon under the bed of phosphor, and (c) with carbon mixed into the raw materials in contrast to the standard patterns of  $\text{SrSi}_2\text{O}_2\text{N}_2$  (ICSD card 76-3141) and  $\text{Sr}_2\text{Si}_5\text{N}_8$  (JCPDS 85-0101). The diffraction peaks in the absence of carbon (Fig. 2(a)) and with phosphor on the bed of carbon (Fig. 2(b)) are indexed to  $\text{SrSi}_2\text{O}_2\text{N}_2$ .<sup>11</sup> However, a certain amount of  $\text{Sr}_2\text{Si}_5\text{N}_8$  in addition to  $\text{SrSi}_2\text{O}_2\text{N}_2$  was observed from Fig. 2(c) with carbon mixing with raw materials. Therefore, the green luminescence with maximum at 534 nm originates from  $\text{SrSi}_2\text{O}_2\text{N}_2:\text{Eu}^{2+}$  and the red luminescence with peak at 632 nm comes from the  $\text{Sr}_2\text{Si}_5\text{N}_8:\text{Eu}^{2+}$ .

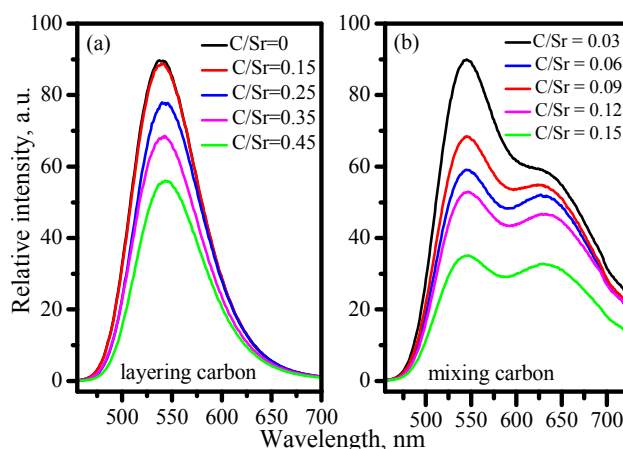


**Fig. 1** Emission phosphors synthesized with different amount of carbon layering at the bottom of crucible (a) and with carbon mixing with raw materials together (b)

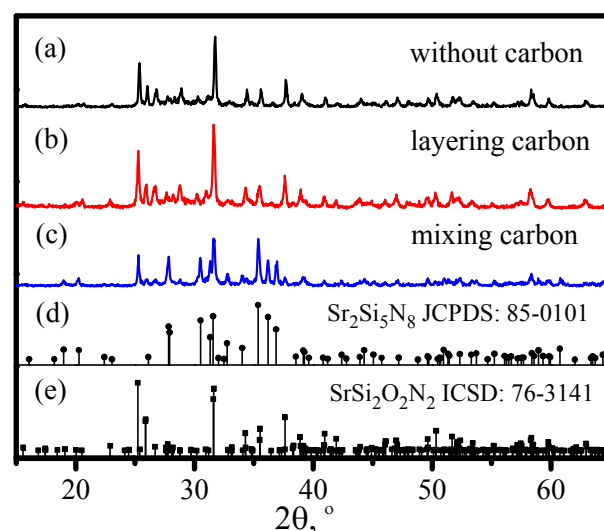


**Fig. 2** The XRD patterns of  $\text{SrSi}_2\text{O}_2\text{N}_2:\text{Eu}^{2+}$  samples synthesized (a) in the absence of carbon, (b) with carbon ( $\text{C}/\text{Sr}=0.15$ ) under the bed of phosphor, and (c) with carbon ( $\text{C}/\text{Sr}=0.15$ ) homogenous mixing with raw materials, compared with the standard XRD patterns of (d)  $\text{Sr}_2\text{Si}_5\text{N}_8$  (JCPDS 85-0101) and (e)  $\text{SrSi}_2\text{O}_2\text{N}_2$  (ICSD card 76-3141)

Evidently in Fig. 1(a), the luminescence intensity of the samples decreases with the increase of carbon, ranging from 0, 0.15, 0.25, 0.35, to 0.45 for the mol ratio of carbon to strontium ( $\text{C}/\text{Sr}$ ) in each sample. It is likely due to the production of higher amounts of nitride phosphor ( $\text{Sr}_2\text{Si}_5\text{N}_8$ ) with the increase of carbon content during synthesis. Although the total area of the emission band which includes the both bands, decreases with the increase of the carbon content from 0.03 M to 0.15 M, the relative ratio of the area of the emission band with peak at 632 nm to the total area of the emission band increases significantly. This phenomenon suggests that a higher quantity of  $\text{Sr}_2\text{Si}_5\text{N}_8:\text{Eu}^{2+}$  is formed when more carbon is mixed into the raw materials. Two phases achieved through two different carbon mixing ways suggest that a close contact of carbon with raw materials is an essential condition for nitride formation.

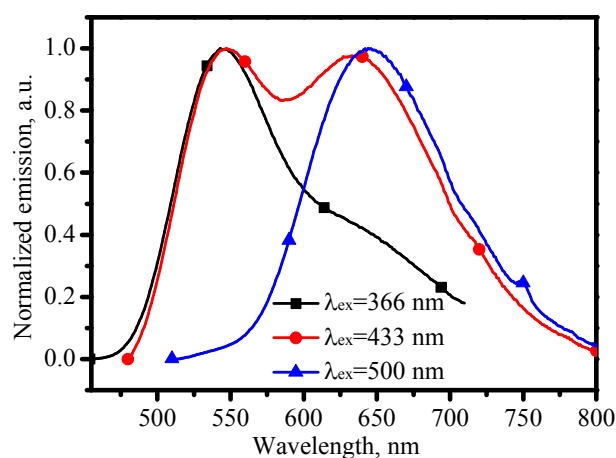


**Fig. 3** Normalized emission spectra of phosphor synthesized by mixing 0.15 M carbon into raw materials excited with 366, 433 and 500 nm

To verify the formation of  $\text{Sr}_2\text{Si}_5\text{N}_8$  phase in this reaction, the phosphor synthesized by mixing with 0.15 M carbon is further characterized by exciting with different wavelengths. The resulting emission spectra with normalized intensities are presented in Fig. 3. On excitation at 366 nm, a dominant green emission with maximum at 545 nm and overlap with a minor asymmetric emission in red region is observed; however, only the red emission band peaked at 632 nm is observed on excitation at 500 nm. When excited by 433 nm, two emission bands are observed simultaneously. The selective excitation further shows that the nitride is formed, because  $\text{SrSi}_2\text{O}_2\text{N}_2:\text{Eu}^{2+}$  is efficiently excited in the near ultraviolet range while  $\text{Sr}_2\text{Si}_5\text{N}_8:\text{Eu}^{2+}$  is sensible to blue.<sup>1, 12</sup>

The nitride phosphor of  $\text{Sr}_2\text{Si}_5\text{N}_8:\text{Eu}^{2+}$  usually was synthesized at 1500 °C or more.<sup>3-9</sup> However, it is observed at the reaction of 1400 °C in this work. To gain insights into this phenomenon, the high resolution Transmission-Electron-Microscope is used to analyze the morphology. As shown in Fig. 4 (a), the phosphor has an irregular rod-like profile. The XRD patterns in Fig. 2 show that the samples crystallize well, either with carbon utilizing or not. However, the amplified image in Fig. 4(b) clearly shows that an amorphous layer (thickness 3-5 nm) is present at the particle surface for the phosphor synthesized by mixing 0.15 M carbon into raw materials. The XRD technique is not sensitive to detect trace of impurity phases, generally no less than 5% weight. However, the high-resolution Transmission-Electron-Microscope is able enough to detect the point lattice of atom arrays. The formation of amorphous layer suggests that a rapid heating and cooling process must have been happened during reaction and the reaction temperature should be higher than melting point.

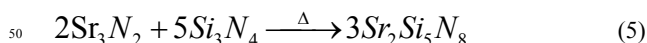
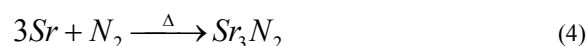
The enthalpy increment of a system over the interval of temperature from  $T_1$  to  $T_2$ , under the constant pressure, usually is described by the expression:<sup>13</sup>

$$\Delta H = \int_{T_1}^{T_2} C_p dT \quad (1)$$

The heat capacity as a function of temperature can be represented by an expression as:<sup>13</sup>

$$C = a + bT + cT^2, \quad (2)$$

where a, b, and c are empirical constants. The heat capacity of  $\text{SrO}$ ,  $\text{C}$  (graphite),  $\text{Sr}$  and  $\text{CO}$  at room temperature ( $T_1=25^\circ\text{C}$ ) are 79.45, 8.517, 26.79, and 29.14 KJ/mol, respectively.<sup>13</sup> Neglecting the change of heat capacity with temperature, there is at least 54595 KJ/mol heat released from the reaction (3) at 1400 °C.



The reaction (4) of metal  $\text{Sr}$  nitridation can happen at low temperature, less 800. The nitride and oxynitride compounds have high capacity but poor thermal conductivity, so the reaction heat can only transfer within a short distance. Much heat released from reaction (3) propagating within local area makes the temperature of regional phosphor higher than the 1400 °C for reaction. Once it exceeds the melt of material, the amorphous phase will be formed during the cooling process. So, the mechanism of amorphous formation can be elucidated with the scheme 1. The heat produced in reaction (3) induces the reaction (5) happened to form the nitride phosphor of  $\text{Sr}_2\text{Si}_5\text{N}_8:\text{Eu}^{2+}$ . It is because of the heat that the nitride compounds are easily synthesized using the CRN route at relatively low temperature.

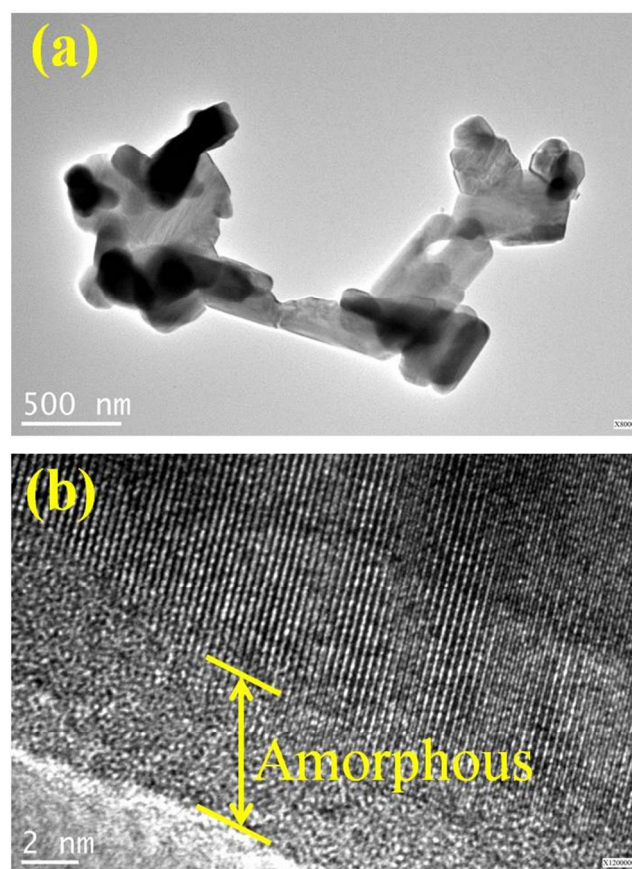
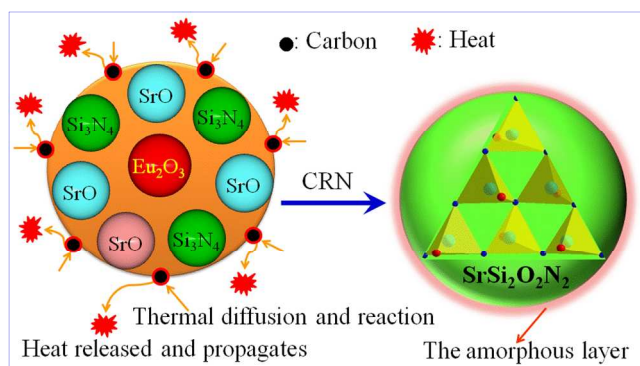


**Fig. 4** TEM picture of the phosphor particles synthesized by mixing 0.15 M carbon into raw materials (a) and its amplified surface profile (b)





**Scheme 1** The mechanism of amorphous phase formation in the CRN route to  $\text{SrSi}_2\text{O}_2\text{N}_2: \text{Eu}^{2+}$

Sakuma et al.<sup>14</sup> demonstrated a warm-white light-emitting diode (LED) without blending of different kinds of phosphors by pre-coating a newly developed yellowish orange  $\text{CaEuSiAlON}$  ceramic phosphor on a blue LED chip, which provides us a good inspiration for the application of the orange phosphor consisting of  $\text{SrSi}_2\text{O}_2\text{N}_2: \text{Eu}^{2+}$  and  $\text{Sr}_2\text{Si}_5\text{N}_8: \text{Eu}^{2+}$ , synthesized by mixing carbon. If the ratio of green to red were reasonably tailored, it is possible to fabricate white LEDs using the individual phosphor. However, the internal and external quantum efficiency, the absorption efficiency, and the thermal stability of luminescence (TSL) are crucial for the applications of phosphor in white LED.

The absorbance and the internal and external quantum efficiency of  $\text{SrSi}_2\text{O}_2\text{N}_2: \text{Eu}^{2+}$  phosphor, synthesized by layering 0.15 M at bottom, are about 87.2%, 103.1% and 89.9%, respectively when excited with 380 nm, as presented in Table 1, indicating that the phosphors are well prepared. With carbon concentration kept at the same level, Table 1 shows that the absorbance and internal and external quantum efficiency of the phosphor synthesized by homogeneous mixing carbon with raw materials together is lower than that by layering carbon at bottom. The low quantum efficiency is caused by too much carbon mixed. From the Fig. 1(b) we can get to know that the quantum efficiency will be high if with much less carbon doped, such as 0.03 M.

**Table 1** The absorbance and the internal and external quantum efficiency (QE) of  $\text{SrSi}_2\text{O}_2\text{N}_2: \text{Eu}^{2+}$  phosphor synthesized by layering 0.15 M at bottom and by mixing 0.15 M carbon into raw materials, respectively, compared with the commercial available  $\text{Y}_3\text{Al}_5\text{O}_{12}: \text{Ce}^{3+}$  (YAG: Ce)

Samples	Excitation wavelength	Absorbance	Internal QE	External QE
$\text{SrSi}_2\text{O}_2\text{N}_2: \text{Eu}^{2+}$ (layering carbon)	380 nm	87.2 %	103.1 %	89.9 %
	433 nm	80.4 %	88.0 %	70.7 %
	455 nm	73.2 %	84.8 %	62.0 %
$\text{SrSi}_2\text{O}_2\text{N}_2: \text{Eu}^{2+}$ (mixing carbon)	380 nm	69.4 %	80.8 %	56.1 %
	433 nm	63.7 %	71.3 %	45.4 %
	455 nm	57.3 %	67.0 %	38.4 %
YAG: Ce (commercial)	455 nm	84.6 %	88.0 %	74.0 %

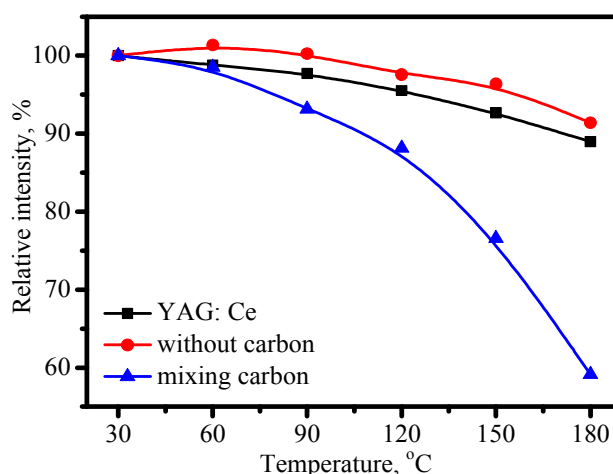


**Fig. 5** The comparison of the thermal stability of the luminescence of the commercially available  $\text{Y}_3\text{Al}_5\text{O}_{12}: \text{Ce}^{3+}$  (YAG: Ce) with the  $\text{SrSi}_2\text{O}_2\text{N}_2: \text{Eu}^{2+}$  synthesized without mixing carbon and by mixing 0.15 M carbon into raw materials

The relative luminescence intensity, determined by integrating emission spectra from 400 to 800 nm and the relative emission intensity at 30 °C was normalized to 100%, as a function of temperature is displayed in Fig. 5, which clearly shows that the phosphor synthesized by layering carbon at bottom has a better performance than the commercial available  $\text{Y}_3\text{Al}_5\text{O}_{12}: \text{Ce}^{3+}$  (YAG: Ce). However, thermal stability of the phosphor synthesized by mixing carbon into raw materials is worse than the YAG: Ce.

The positive effect of carbon in contributing to the formation of nitride compound is solid. However, the negative effect of the carbon brought on quantum efficiency and the thermal stability of luminescence is also substantial. In order to avoid the negative and make full of the positive effect, the carbon particles used to synthesize phosphor should as fine as possible, so as to reduce the amount of heat released per unit. Accordingly, the amorphous phase due to the heat that cannot propagate efficiently and result in an increase of temperature in local area will decrease.

## Conclusion

The carbothermal reduction and nitridation (CRN) reaction route were intended to synthesize the nominal phosphor of  $\text{SrSi}_2\text{O}_2\text{N}_2: \text{Eu}^{2+}$  at a relative lower temperature of 1400 °C than that required for lower  $\text{Sr}_2\text{Si}_5\text{N}_8: \text{Eu}^{2+}$ . However, the  $\text{Sr}_2\text{Si}_5\text{N}_8: \text{Eu}^{2+}$  was obtained in addition to  $\text{SrSi}_2\text{O}_2\text{N}_2: \text{Eu}^{2+}$ . This work firstly approves that the carbothermal reduction indeed affords nitride compound. Through analysis of the two different pathways of carbon mixing on objective products, the work demonstrates that a close contact of carbon with raw materials, used to conduct heat, is an essential condition for nitride formation. The presence of an amorphous layer on the surface of phosphor particles, observed by HR-TEM, suggests that a rapid heating and cooling process happened during reaction and the temperature of local area should be higher than the melt point. Whereby, we can give a reasonable explanation to the mechanism of carbothermal reduction contributed to nitride formation at relatively low

temperature, i.e., the heat released from carbothermal reduction reaction propagates within local region makes the temperature of phosphor much higher than the theoretic temperature of reaction, and essentially promotes the nitridation reaction to form  $\text{Sr}_2\text{Si}_5\text{N}_8$ :

$5 \text{ Eu}^{2+}$ .

## Acknowledgments

The work was supported by the National High-Tech R&D Program (National 863 program) (2013AA03A114), the National Natural Science Foundation (51002043 and U1332133), the Science and Technology Program of Anhui Province (12010202004, 1301022062, and 1301022067), the China Postdoctoral Science Foundation (2012T50568). Moreover, the authors appreciate Dr. Ronghui Liu, a senior scientist at Grirem Advanced Materials Co., Ltd, for his help measure the quantum efficiency.

## Notes and references

- <sup>a</sup> School of Materials Science and Engineering, Hefei University of Technology, Hefei 230009, China. Email: shanggan2009@qq.com (L. Chen) and lhqjs@hfut.edu.cn (H. Li).
- <sup>b</sup> Department of Chemistry, Anhui Science and Technology University, Fengyang 233100, China. chshifu@chnu.edu.cn.
- <sup>c</sup> Center of Analysis and Measurement, Hefei University of Technology, Hefei 230009, China.
- 1 L. Chen, C.C. Lin, C.W. Yeh, R.S. Liu, *Mater.*, 2010, **3**, 2172.
  - 2 Chongfeng Guo, Heng Jing and Ting Li, *RSC Adv.*, 2012, **2**, 2119.
  - 3 Takayuki Suehiro, Rong-Jun Xie, Naoto Hirosaki, *Industry and Engineering Chemistry Research*, 2013, **52**(22), 7453-7456.
  - 4 Hui-Li Li, Rong-Jun Xie, Naoto Hirosaki, and Takashi Takeda, Guohong Zhou, *Int. J. Appl. Ceram. Technol.*, 2009, **6**(4), 459.
  - 5 Y. Q. Li, G. de With, H. T. Hintzen, *J. Solid State Chem.*, 2008, **181**, 515.
  - 6 Rong-Jun Xie, Naoto Hirosaki, Takayuki Suehiro, Fang-Fang Xu, Mamoru Mitomo, *Chem. Mater.* 2006, **18**, 5578.
  - 7 Kang Sik Choi, Soon Duk Jee, Jung Pyo Lee, *Journal of Nanoscience and Nanotechnology* 2013, **13**(3), 1867.
  - 8 Xianqing Piao, Takashi Horikawa, Hiromasa Hanzawa, Ken-ichi Machida, *Appl. Phys. Lett.* 2006, **88**, 161908.
  - 9 Xianqing Piao, Takashi Horikawa, Hiromasa Hanzawa, Ken-ichi Machida, *J Electrochem Soc*, 2006, **153**(12), H232.
  - 10 Y. Kim, J. Kim, S. Kang, *J. Mater. Chem. C* 2013, **1**, 69.
  - 11 M. Seibald, T. Rosenthal, O. Oeckler, F. Fahrnbauer, A. Tücks, P. J. Schmidt, W. Schnick, *Chem. Eur. J.*, 2012, **18**, 13446.
  - 12 J. Ruan, R. J. Xie, N. Hirosaki, T. Takeda, *J. Electrochem. Soc.*, 2012, **159**, H66.
  - 13 J. G. Speight, Lange's Handbook of Chemistry, in section 6, thermodynamic properties, McGraw-Hill Professional (1th edition), 1998. E. F. Schubert, J. K. Kim, *Science*, 2005, **308**, 1274.
  - 14 K. Sakuma, K. Omichi, N. Kimura, M. Ohashi, D. Tanaka, N. Hirosaki, Y. Yamamoto, R. J. Xie, and T. Suehiro, *Optic. Lett.* 2004, **29** (17), 2001.